Palaeoentomology 009 (2): 125–138
https://www.mapress.com/pe/

Article

ISSN 2624-2826 (print edition)
PALAEOENTOMOLOGY
ISSN 2624-2834 (online edition)

https://doi.org/10.11646/palaeoentomology.9.2.5
http://zoobank.org/urn:lsid:zoobank.org:pub:8FF1CD84-FB7E-403A-9D59-8290AF3E01A6

Cretolala kachinensis gen. et sp. nov. (Hemiptera: Fulgoromorpha: Delphacoidea), the first lalacid from mid-Cretaceous Kachin amber: morphological and taphonomic implications

YA-NI TANG[1, 2, 3], LUCIA ŠMÍDOVÁ[4], YING-YING DING[5], MATHIEU BODERAU[6], DOLEV FABRIKANT[7], BASTIAN MÄHLER[3], JUN-CHEN DENG[8, 9], THET TIN NYUNT[10], YAN-ZHE FU[11], CORENTIN JOUAULT[12], FRANK TOMASCHEK[13], JACEK SZWEDO[14] & HUI JIANG[3, 11, 15, *]

[1]*Yunnan Key Laboratory for Palaeobiology, Institute of Palaeontology, Yunnan University, South Waihuan Road, Chenggong District, Kunming 650500, China*
[2]*MEC International Joint Laboratory for Palaeobiology and Palaeoenvironment, Yunnan University, Kunming 650500, China*
[3]*Bonn Institute for Organismic Biology (BIOB), Department for Paleontology, University of Bonn, Bonn 53115, Germany*
[4]*Institute of Rock Structure and Mechanics of the Czech Academy of Sciences, V Holešovičkách 41, 18200, Prague, Czech Republic*
[5]*Institute of Physiology II, University Hospital Bonn, University of Bonn, 53115 Bonn, Germany*
[6]*Institut de Systématique, Évolution, Biodiversité (UMR 7205), Muséum national d'Histoire naturelle, CNRS, Sorbonne Université, EPHE-PSL, Université des Antilles, Paris F-75005, France*
[7]*The Steinhardt Museum of Natural History and The New Environmental School, Tel Aviv University, 69978 Tel Aviv, Israel*
[8]*Natural History Museum of Denmark, University of Copenhagen, Copenhagen 1350, Denmark*
[9]*Institute of Environmental Sciences, Faculty of Biology, Jagiellonian University, Kraków, Poland*
[10]*Department of Geological Survey and Mineral Exploration, Ministry of Natural Resources and Environmental Conservation, Myanmar Gems Museum, Nay Pyi Taw 15011, Myanmar*
[11]*State Key Laboratory of Palaeobiology and Stratigraphy, Nanjing Institute of Geology and Palaeontology, Chinese Academy of Sciences, Nanjing 21008, China*
[12]*Oxford University Museum of Natural History, University of Oxford, Parks Road, Oxford OX1 3PW, UK*
[13]*Institute of Geosciences, University of Bonn, Bonn 53115, Germany*
[14]*Laboratory of Evolutionary Entomology and Museum of Amber Inclusions, Department of Invertebrate Zoology and Parasitology, University of Gdańsk, Gdańsk, PL80–308, Poland*
[15]*Institute of Geology and Paleontology, Charles University, Prague 12843, Czech Republic*
yani_0304@126.com; https://orcid.org/0000-0002-2716-3315
luciasmidova1@gmail.com; https://orcid.org/0000-0002-5798-7817
Yingying.ding@ukbonn.de; https://orcid.org/0000-0001-9644-7461
mathieu.boderaul@mnhn.fr; https://orcid.org/0000-0001-7088-9560
Dolevf@mail.tau.ac.il; https://orcid.org/0009-0004-4388-4026
bastian.maehler@uni-bonn.de; https://orcid.org/0000-0002-0993-8578
jd@snm.ku.dk; https://orcid.org/0000-0003-3669-7172
thettinnyunt@gmail.com; https://orcid.org/0000-0002-6252-0488
yzfu@nigpas.ac.cn; https://orcid.org/0000-0002-7819-1703
joualtc0@gmail.com; https://orcid.org/0000-0002-3680-5172
ftom@uni-bonn.de; https://orcid.org/0000-0002-8284-7736
jacek.szwedo@ug.edu.pl; https://orcid.org/0000-0002-2796-9538
hui.jiang@uni-bonn.de, huijiang2353@163.com; https://orcid.org/0000-0002-7873-5213
**Corresponding author*

Abstract

We report *Cretolala kachinensis* **gen. et sp. nov.**, the first formally described representative of the family Lalacidae from mid-Cretaceous (~99 Ma) Kachin amber. The morphology and taphonomy of the specimen were studied using optical microscopy, micro-computed tomography (micro-CT), confocal laser scanning microscopy (CLSM), and scanning electron microscopy coupled with energy-dispersive X-ray spectroscopy (SEM–EDS). *Cretolala kachinensis* **gen. et sp. nov.** exhibits a unique combination of forewing characters, including a strengthened, broad, and wrinkled costal margin; ScP+R fork proximal to both the Pcu+A_1 fusion and the CuA fork; MP with five terminals; and CuA_1 and CuA_2 each with two terminals. Crossvein patterns differ between the left and right forewings, indicating that crossvein expression alone is not diagnostic. The forewing bears distinct maculation, with a face-like pattern dorsally and an extensive lateral pattern that may indicate aposematism, mimicry, or plant-like camouflage in

Submitted: 19 Dec. 2025; accepted by D.-Y. Huang: 8 Apr. 2026; published: 29 Apr. 2026

an arboreal herbivore. Taphonomic analyses based on optical micrographs and material-dependent X-ray attenuation in micro-CT show that minerals are distributed throughout the fossil, coating anatomical surfaces and infilling pre-existing cavities and voids. These phases help stabilize morphology and influence the micro-CT reconstruction of soft-bodied structures. SEM–EDS analyses indicate that the body-coating and void-filling minerals are dominated by quartz and pyrite, with feldspars and aluminosilicate mixtures also present, locally enriched in K, Na, Mg, or Ca. This assemblage and its textures point to a polyphase paragenetic sequence, with early detrital infill and later authigenic mineralization. Our results suggest that minerals and some chemicals derived from the host sediments can be transported into and, in some cases, precipitated within amber inclusions, infilling voids and providing structural support that influences fossil preservation. Collectively, these phases occlude porosity, stabilize morphology, and enhance X-ray contrast, although they locally obscured primary tissue boundaries. Our results highlight multistage diagenesis in Kachin amber and underscore variability among inclusions in both mineral assemblages and the timing of mineralization/diagenetic events.

Keywords: Mesozoic, Burmese amber, planthopper, taxonomy, taphonomy, mineral infilling, wing maculation

Introduction

Lalacidae is an extinct family of planthoppers established by Hamilton (1990). The family was described on the basis of compression fossils from the Aptian Konservat-Lagerstätte of the Nova Olinda Member (Crato Formation) in the Araripe Basin, northeastern Brazil (Hamilton, 1990; Szwedo, 2007). Currently, the family comprises 11 genera and 21 species (Ren *et al*., 1998; Szwedo *et al*., 2004; Bucher *et al*., 2024; Boderau *et al*., 2025a). Most of these fossil records are Aptian in age, with only one species known from the Barremian (Fig. 1A, B) (Ren *et al*., 1998; Szwedo *et al*., 2004; Bucher *et al*., 2024).

Eight genera are known from the Crato Formation of Brazil and are assigned to three subfamilies and five tribes: Ancoralinae Hamilton, 1990, comprising two tribes, Ancoralini Hamilton, 1990 and Kinnarocixiini Hamilton, 1990; Protodelphacinae Hamilton, 1990, comprising Protodelphacini Hamilton, 1990; and Lalacinae Hamilton, 1990, comprising two tribes, Lalacini Hamilton, 1990 and Carpopodini Hamilton, 1990 (Hamilton, 1990; Szwedo *et al*., 2004; Bucher *et al*., 2024; Bourgoin, 2025). Three genera are known from the Cretaceous of East Asia: *Yanducixius* Ren *et al*., 1995 and *Cretocixius* Zhang, 2002 from the Lushangfen Formation, China, and *Lapicixius* Ren *et al*., 1998 from the Yixian Formation, Liaoning, China; none of which are currently assigned to any subfamily or tribe within Lalacidae (Ren *et al*., 1998; Szwedo *et al*., 2004; Bucher *et al*., 2024). Sixteen fossil species from the Crato Konservat-Lagerstätte in the Southern Hemisphere exhibit high morphological disparity and taxonomic diversity, whereas only five species are currently known from China in the Northern Hemisphere (Fig. 1A, B) (Ren *et al*., 1998; Szwedo *et al*., 2004; Bucher *et al*., 2024; Boderau *et al*., 2025a).

Regarding the origin of Lalacidae, Bucher (2024) used total-evidence dating approach to infer a Late Jurassic–Early Cretaceous origin, with median age estimates of *ca*. 148–133 Ma. More recent fossil-based estimates suggest an Early Cretaceous origin, with a root age of *ca*. 123 Ma (Boderau *et al*., 2025b). Given the still-evolving taxonomic framework and ongoing methodological advances, robust phylogenetic reconstruction of Lalacidae requires the discovery of additional, better-preserved specimens and a more systematic assessment of the fossil record.

Most described species are largely based on incomplete specimens, the concept and circumscription of the family Lalacidae remain unclear (Bourgoin & Szwedo, 2022, 2023; Bucher *et al*., 2024). The diagnosis of the family Lalacidae provided by Hamilton (1990) is relatively broad and does not fully clarify its separation from other cixiid-like groups. However, Lalacidae can be distinguished by a combination of features: (i) a relatively broad and wrinkled appendix of forewing; (ii) stem CuA forked once in prenodal region, and both branches CuA_1 and CuA_2 forked again before reaching wing margin; (iii) metatibial spiniform sensilla not developed or absent, but metatibial subapical platellae present; (iv) basimetatarsomere subequal in length to combined length of middle and distal metatarsomeres; (v) head capsule with coryphe, acrometope, and eumetope separated by transverse carinae, and with lateral carinae of metope and postclypeus elevated; (vi) a collar-like pronotum; and (vii) an orthopteroid-type ovipositor, relatively short, strongly curved, sword-shaped and apically rounded.

Here, we describe the first representative of Lalacidae from the 'mid'-Cretaceous (~99 Ma) amber of Kachin, Myanmar. This record documents the third known fossil locality of Lalacidae in the Northern Hemisphere and the first occurrence from Southeast Asia (Fig. 1C). The new specimen is also the first amber-preserved representative of the family, expanding the known morphological diversity and taphonomic breadth of the group.

Beyond its morphological features, the specimen is taphonomically informative: detrital and authigenic mineral precipitates coat external surfaces and infill internal cavities. We characterized these phases using scanning electron microscopy with energy-dispersive X-ray spectroscopy (SEM–EDS). Consistent with recent studies proposing multiple episodes of fluid ingress modulating inclusion preservation in Kachin amber (*e.g*., Jiang *et al*., 2022; Stagg *et al*., 2026), our

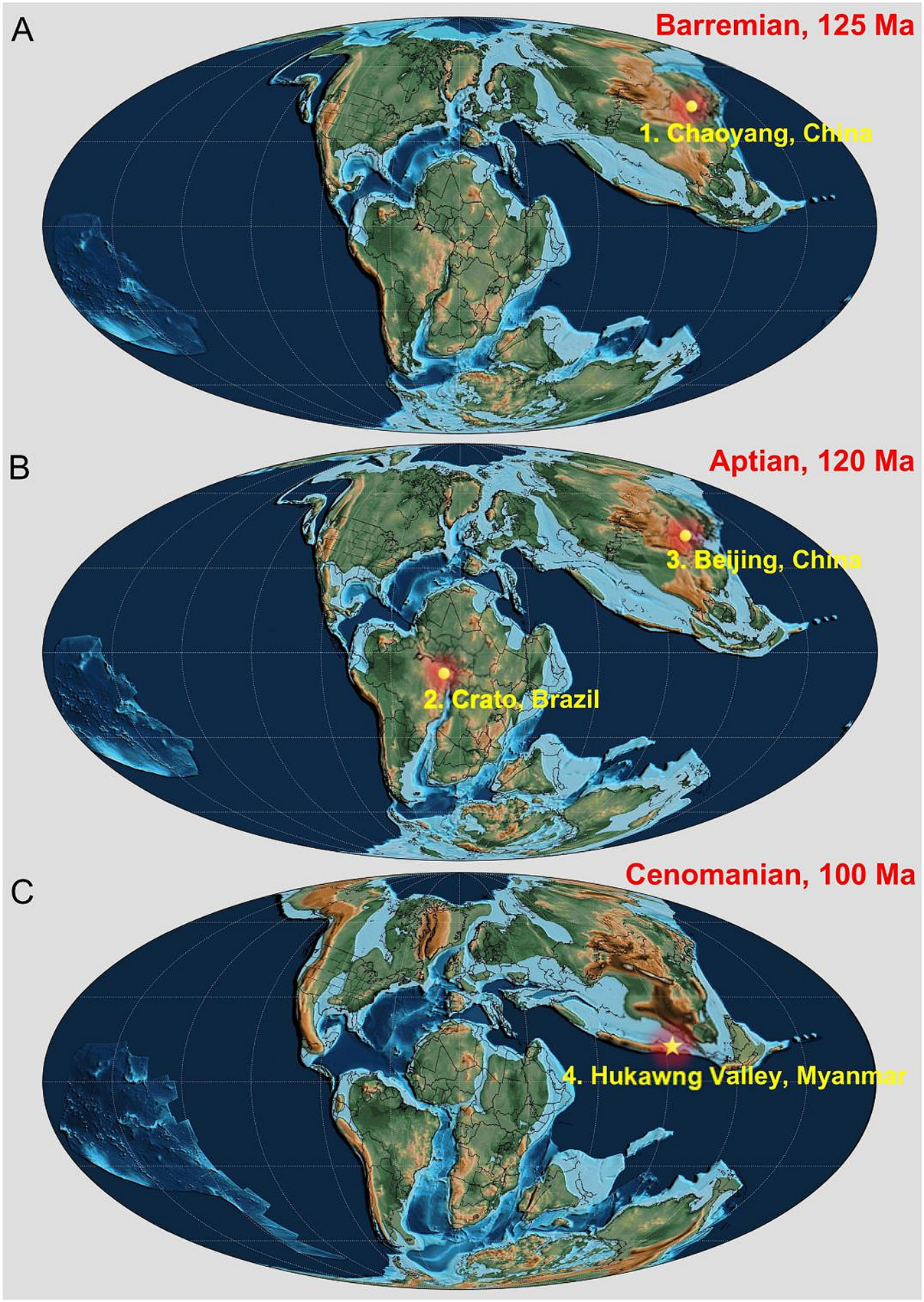

FIGURE 1. Paleogeographic distribution of Lalacidae fossil localities. **A**, Barremian, 125 Ma of the map: 1, Yixian Formation, Chaoyang area, northeastern China. **B**, Aptian, 120 Ma of the map: 2, Crato Formation, Crato, northeastern Brazil; 3, Lushangfen Formation, Beijing area, northern China. **C**, Cenomanian, 100 Ma of the map: 4, Kachin amber, Hukawng Valley near Tanai, northern Myanmar. (Map source: Scotese *et al*., 2025).

analyses support a multistage diagenetic model and indicate that differences in specimen preservation reflect microtaphonomic heterogeneity in fluid chemistry and burial conditions.

Material and methods

The amber specimen originates from a site (approximately 26°15′N, 96°34′E) in Hukawng Valley, Tanaing Township, Myitkyina District, Kachin State, Myanmar (Thu & Zaw, 2017). The geographical coordinates of the site are approximately 26°15′ N, 96°34′ E. The specimen will be permanently deposited in Myanmar Gems Museum, Nay Pyi Taw, Myanmar, upon completion of this study. The age of Hukawng amber is 98.8 ± 0.6 Ma, according to U-Pb dating of zircons from the volcanoclastic matrix (Shi *et al*., 2012). The amber piece, HMJ–2016–019, was collected between 2013 and 2016, well before the Myanmar army closed the Kachin amber mines in November 2017. The fossil was acquired in full compliance with the laws of Myanmar, and with the International Code of Zoological Nomenclature (ICZN, 1999), Statement of the International Palaeoentomological Society (Szwedo *et al*., 2020), and the policies proposed by Haug *et al*. (2020).

Reflected-light micrographs were acquired using a Zeiss AXIO ZoomV16 stereomicroscope at the Bonn Institute of Organismic Biology, Section Paleontology, University of Bonn. Each image represents a digitally stacked composite of ~15–50 photographs taken at different focal planes and combined using Helicon Focus v7.

Micro-CT data were acquired using a Phoenix V|tome|x S 180 micro-CT (GE Measurement and Control, Wunstorf, Germany) located at the Bonn Institute of Organismic Biology, Section Paleontology, University of Bonn, using a DXR-250 flat-panel detector (2024 × 2024 px, 16-bit) at 80 kV and 80 µA, 500 ms per projection, with 1000 projections over 360°, yielding an isotropic voxel size of 6.70 µm (0.00670448 mm). Volume data processing was performed using the software Avizo 8.1 (FEI Visualization Sciences Group).

Backscattered electron (BSE) imaging and energy-dispersive X-ray spectroscopy (EDS) analyses were conducted at the Bonn Institute of Organismic Biology (BIOB), University of Bonn, using a TESCAN VEGA 4 scanning electron microscope equipped with a tungsten filament and a TESCAN Essence™ energy-dispersive X-ray spectroscopy (EDS) system. Prior to analysis, samples were carbon-coated using a Quorum Q150T ES sputter coater (Quorum Inc., Lewes, UK). Observations were performed at an accelerating voltage of 15 kV and a working distance of 10 mm.

Confocal z-stacks were acquired on a Nikon A1 confocal laser scanning microscope with the LFOV (FOV25) head mounted on a Ti2 inverted microscope at the Anatomical Institute of the University of Bonn. Excitation used the 488-nm laser line; fluorescence was detected on GaAsP PMTs (DU4) after a 405/488/561/640 dichroic and a 525/50-nm band-pass emission filter. A Nikon Plan 4×/0.10 NA air objective (n = 1.00) was used, with the confocal pinhole set to 20.4/21.7 µm. Images were recorded at 1024 × 1024 pixels with scanner zoom 0.720–4.000. Line averaging was set to 4 with one-way Galvano scanning. Each dataset comprised a single channel (Alexa Fluor 488) Z-stack of 7–90 optical sections at 5-µm spacing. Data were saved as 12-bit ND2 files (stored as 16-bit in memory). Images were viewed and measured in Fiji/ImageJ (v2.16.0/1.54p).

Systematic framework for Fulgoromorpha Evans, 1946 follows Bucher *et al*. (2024) and Bourgoin & Szwedo (2023); genitalic terminology follows Bourgoin (1993); wing venation terminology follows Nel *et al*. (2012) and Bourgoin *et al*. (2015), adapted by Schubnel *et al*. (2019) for the postcubitus vein. Wing venation abbreviations as follows: C, costa; ScP, subcostal posterior; RA, radius anterior; RP, radius posterior; MP, media posterior; $CuA_{1,}$ first branch of cubitus anterior; $CuA_{2,}$ second branch of cubitus anterior; CuP, cubitus posterior; Pcu, postcubitus vein; $A_{1,}$ first anal vein. Crossveins are written in lower-case (*e.g*., mp-cu_1 crossvein between MP_{4+5} and CuA_1 or posterior margin of wing).

Systematic palaeontology

Order Hemiptera Linnaeus, 1758
Suborder Fulgoromorpha Evans, 1946
Superfamily Delphacoidea Leach, 1815
Family Lalacidae Hamilton, 1990

***Cretolala* Jiang, Boderau, Jouault & Szwedo gen. nov.**
LSID urn:lsid:zoobank.org:act:229091A3-D052-4B1E-B472-30CE7D06F45

Type species. *Cretolala kachinensis* **sp. nov.**; by present designation and monotypy.

Etymology. The generic name is formed from the combination of "Cretaceous" and generic name "*Lalax*"; the latter is derived from the Greek λάλαξ ("croaker", "caller"), in reference to a lalacid planthopper from the Cretaceous. Gender is feminine.

Diagnosis (provisional, pending confirmation from additional specimens and in combination with species-level diagnostic characters). Tegmen with narrow base and distinctly widened apical portion; costal margin

strengthened, broad and wrinkled. Pc+CP shifted away from anterior margin near tegmen base, parallel to CA, forming a narrow, sclerotized costal area. ScP+R forks basad both CuA fork and Pcu+A_1 fusion. RA with two terminals; RP with three terminals; MP with five terminals; CuA_1 and CuA_2 with two terminals each.

***Cretolala kachinensis* Jiang, Boderau, Jouault & Szwedo sp. nov.**

LSID urn:lsid:zoobank.org:act:229091A3-D052-4B1E-B472-30CE7D06F45

(Figs 2–5)

Material. Holotype: HMJ–2016–019, adult female in Kachin (Burmese) amber from northern Myanmar. Repository: Myanmar Gems Museum, Nay Pyi Taw, Myanmar. Condition: the specimen is incomplete, with the head and the dorsal part of the thorax missing.

Etymology. The specific epithet is derived from "Kachin", the name of the state in northern Myanmar where the amber originates, and is Latinized with the adjectival suffix *-ensis*, meaning from "Kachin".

Diagnosis. As for the genus, due to monotypy. Additional features include forewing coloration and venation details: costal margin with a continuous dark band along costal area; membrane bearing nearly continuous aligned patches and short transverse bands; a discrete insular macula on ScP+RA; a sub-elliptical isolated macula near distal Pcu; distad of forks of RP and MP, pigment is vein-following, tracking adjacent longitudinal and crossveins; postnodal cell centers unpigmented, forming hyaline "windows"; cell C1 wider than cells C3 and C5, cell C3 about as long as cell C5; metatibiotarsal formula 5:8:14, subapical platellae (sarcochaetae) not observed, possibly absent; gonapophysis IX with distinct apical serrations.

Locality and horizon. Noije Bum Hill, Hukawng Valley, Kachin State, Myanmar; mid-Cretaceous, Cenomanian.

Description. Head and dorsum of thorax not preserved (Fig. 2).

Forewing (Tegmen) (Fig. 3). Basal portion missing; preserved length about 6.6 mm, width about 4.1 mm; membranous; corium narrowing towards base, membrane widening posteriad; tornus straight, not convex, as a prolongation of claval margin; anteroapical angle widely rounded, at the same level as posteroapical angle; posteroapical angle rounded; costal margin blade-shaped, with a distinct, sclerotized costal area formed between costal margin (CA) and praecosta+costa posterior (Pc+CP); costal weakening at level of stigmal area (damaged); ambient vein distinct, appendix wide, transversely wrinkled; clavus with obtuse apex, slightly exceeding ⅔ of tegmen length; basal cell not preserved; preserved stem ScP+R about as long as branch RP to the level of nodal *r-m*$_1$ veinlet, forked basad of CuA forking; branch ScP+RA subparallel to costal margin, ScP forked at the level of nodal *r-m*$_1$ veinlet; postnodal section of RA slightly curved medially, reaching margin at anteroapical angle with two terminals visible; preserved portion of stem MP with a long stalk, first fork at level of nodal line, at level of ScP forking, and apicad of CuA fork, well basad of claval apex; branch MP forked into MP_{1+2} and MP_{3+4} at around level of claval apex, branch MP_{1+2} forked slightly basad of apical line *ir* veinlet, reaching margin with three terminals at apex of forewing; branch MP_{3+4} forked on membrane, apicad of apical line veinlet *m-cu*$_2$, basad of apical line veinlet *im*$_2$; stem CuA forked at level of Pcu+A_1 fusion, branch CuA_1 forked apicad of *m-cu*$_1$ veinlet, reaching margin at posteroapical angle with two terminals, branch CuA_2 forked slightly basad of claval apex, slightly basad of apical *icua* veinlet, reaching margin of tegmen on tornus with two terminals; claval vein CuP bent at apical section, forming obtuse angled apex of clavus; claval vein Pcu slightly sinuate, fused with A_1 apicad of stem ScP+R fork, at level of CuA fork; Pcu+A_1 reaching claval margin with arcuate terminal section, well basad of claval apex; single claval veinlet *cup-pcu* present, placed basad of claval veins junction (tentatively identified; confirmation requires additional material); *icu* veinlet present reaching margin at apex of clavus (tentatively identified; confirmation requires additional material); cell C1 lanceolate, widest at median portion, closed posteriorly with apical line veinlet *ir*; cell C3 about as long as cell C5, cell C3a elongate triangular, both C3 and C3a closed with apical line *imp* veinlets; cell C5 lanceolate, about 5.5 times as long as wide. An additional crossvein *im*$_3$ between MP_3 and MP_4 in left forewing with no counterpart in right forewing; *mp-cua*$_3$ present between MP_4 and CuA_1 in left forewing, with no counterpart in right forewing.

Hind wing (Fig. 3). Right hind wing partly preserved; broad brown marginal band present; RP pectinate, forking into terminals RP_1, RP_2 and RP_3, reaching wing margin at anteroapical angle; preserved portion of MP with two terminals reaching margin; long veinlet *r-m* partly preserved, longer than section of RP apicad veinlet up to fork.

Leg (Fig. 4). Prothoracic legs. Left: tibia partially preserved; tarsi three-segmented; protarsal claws distinct, arolium wide, lobate; right: protibia length about 1.5 mm; protarsus preserved, length about 0.7 mm. Mesothoracic legs. Left: mesocoxa, mesotrochanter, mesofemur partly preserved; mesotibia length about 1.8 mm, with margins covered with lateral microsetae; mesotarsus three-segmented; one preserved mesotarsal claw visible. Right: mesotrochanter, mesofemur, mesotibia, mesotarsomeres partly preserved. Metathoracic legs. Left: metacoxa and metatrochanter partly visible; metacoxa without coxal spine; metafemur length about 1.0 mm, metatibia length

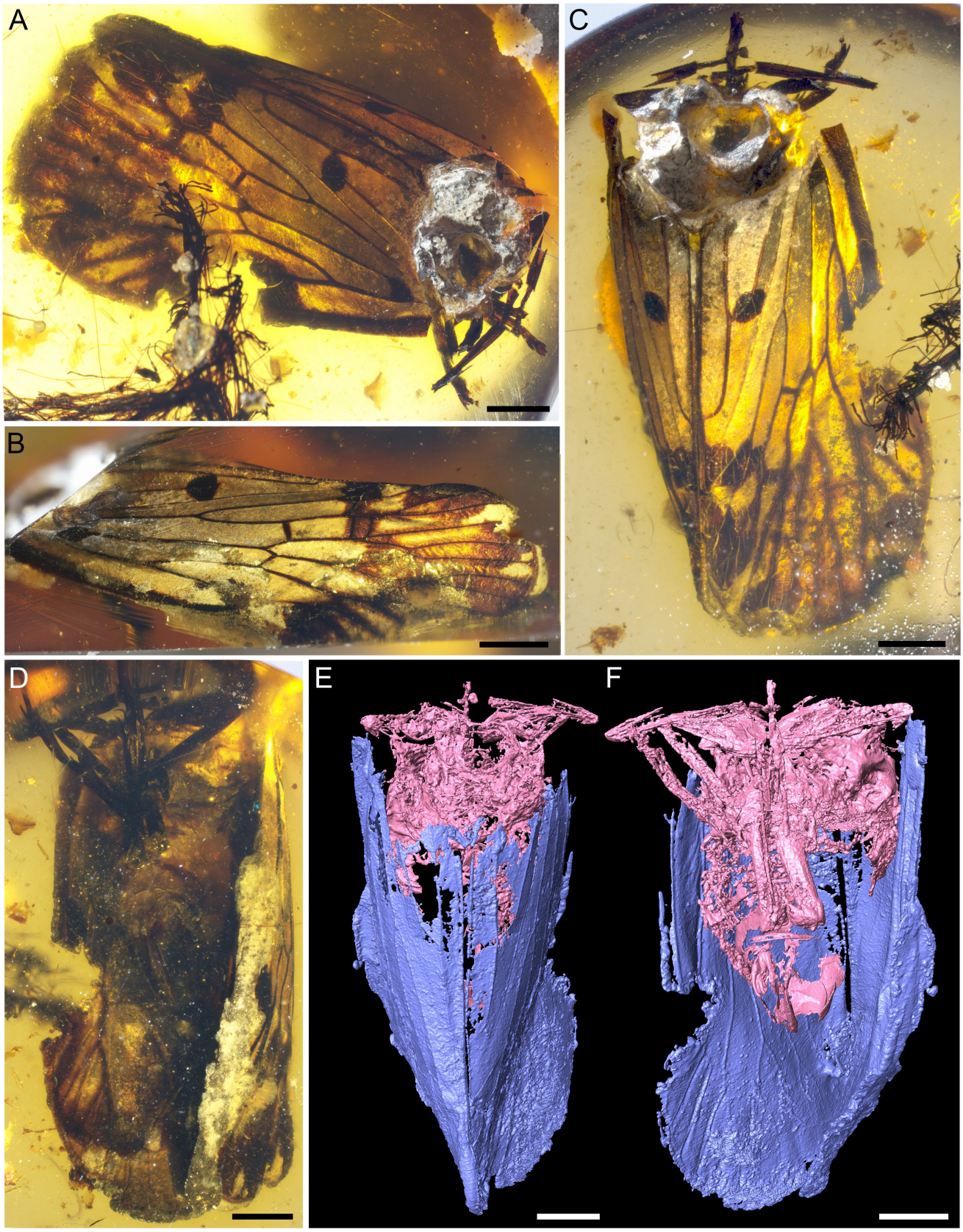

FIGURE 2. *Cretolala kachinensis* **gen. et sp. nov.**, holotype (HMJ–2016–019). **A**–**D**, Reflected-light micrographs. **A**, Right lateral view. **B**, Left lateral view. **C**, Dorsal view. **D**, Ventral view. **E**, **F**, Micro-computed tomography (micro-CT) reconstructions. **E**, Dorsal view. **F**, Ventral view. Scale bars = 1 mm.

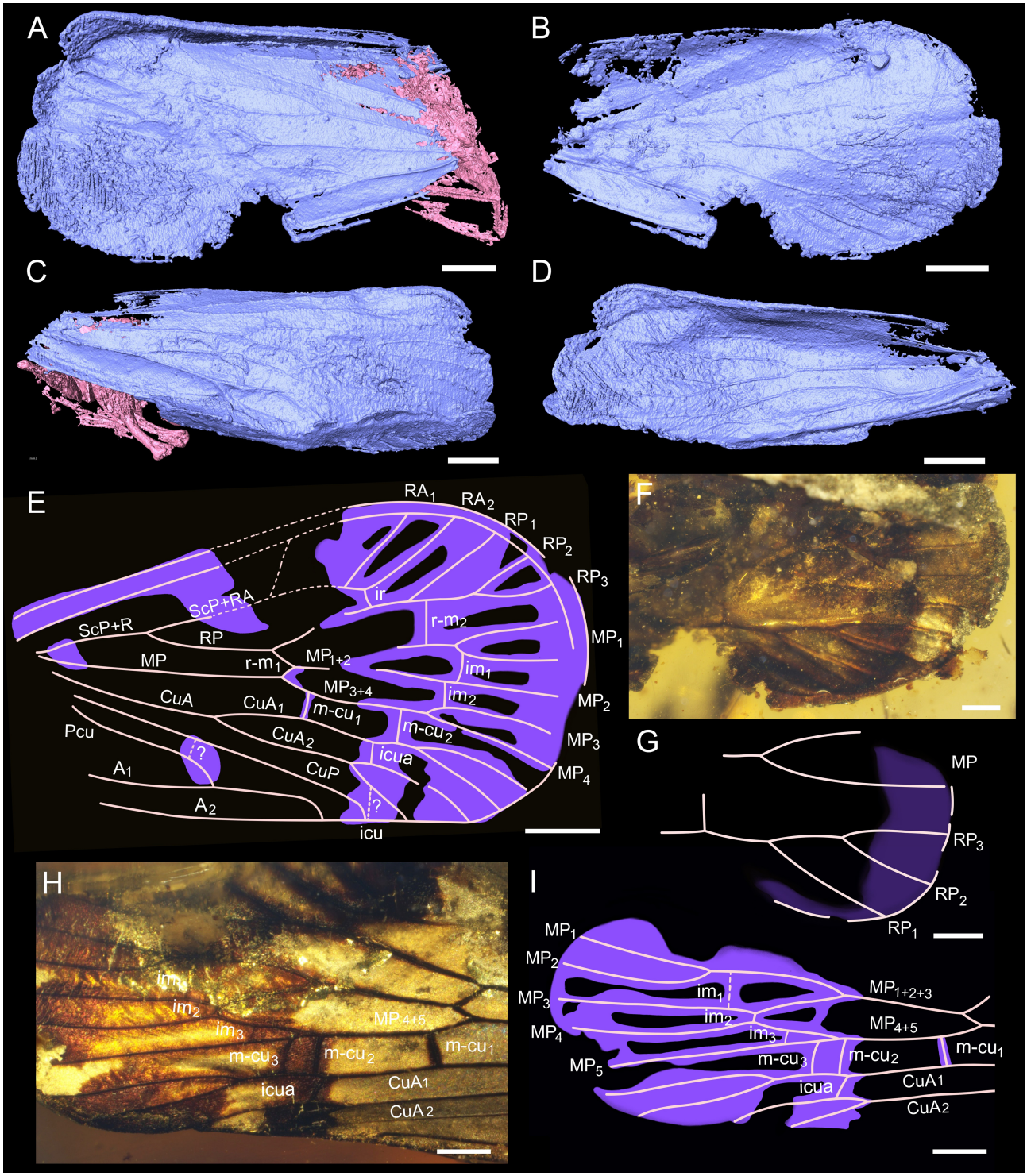

FIGURE 3. Wing venation of *Cretolala kachinensis* **gen. et sp. nov.**, holotype (HMJ–2016–019). **A**–**D**, Micro-CT reconstructions: **A**, Right forewing, external surface; **B**, Right forewing, internal surface; **C**, Left forewing, external surface; **D**, Left forewing, internal surface. **E**, Interpretive drawing of forewing. **F**, Portion of right hind wing, internal surface, reflected-light micrograph. **G**, Overlay drawing corresponding to **F**. **H**, Portion of left forewing showing crossvein differences relative to right forewing, reflected-light micrograph. **I**, Overlay drawing corresponding to **H**. Scale bars = 1 mm (**A**–**E**, **H**, **I**), 0.5 mm (**F**, **G**).

about 1.9 mm, without lateral cuticular spines or metatibial spiniform sensillum visible, with five strong apical teeth; basimetatarsomere length about 1.0 mm, with dense small spines and one lateral long robust spine. Right: metafemur partly preserved; metatibia with three apical spines visible; metabasitarsomere partly preserved.

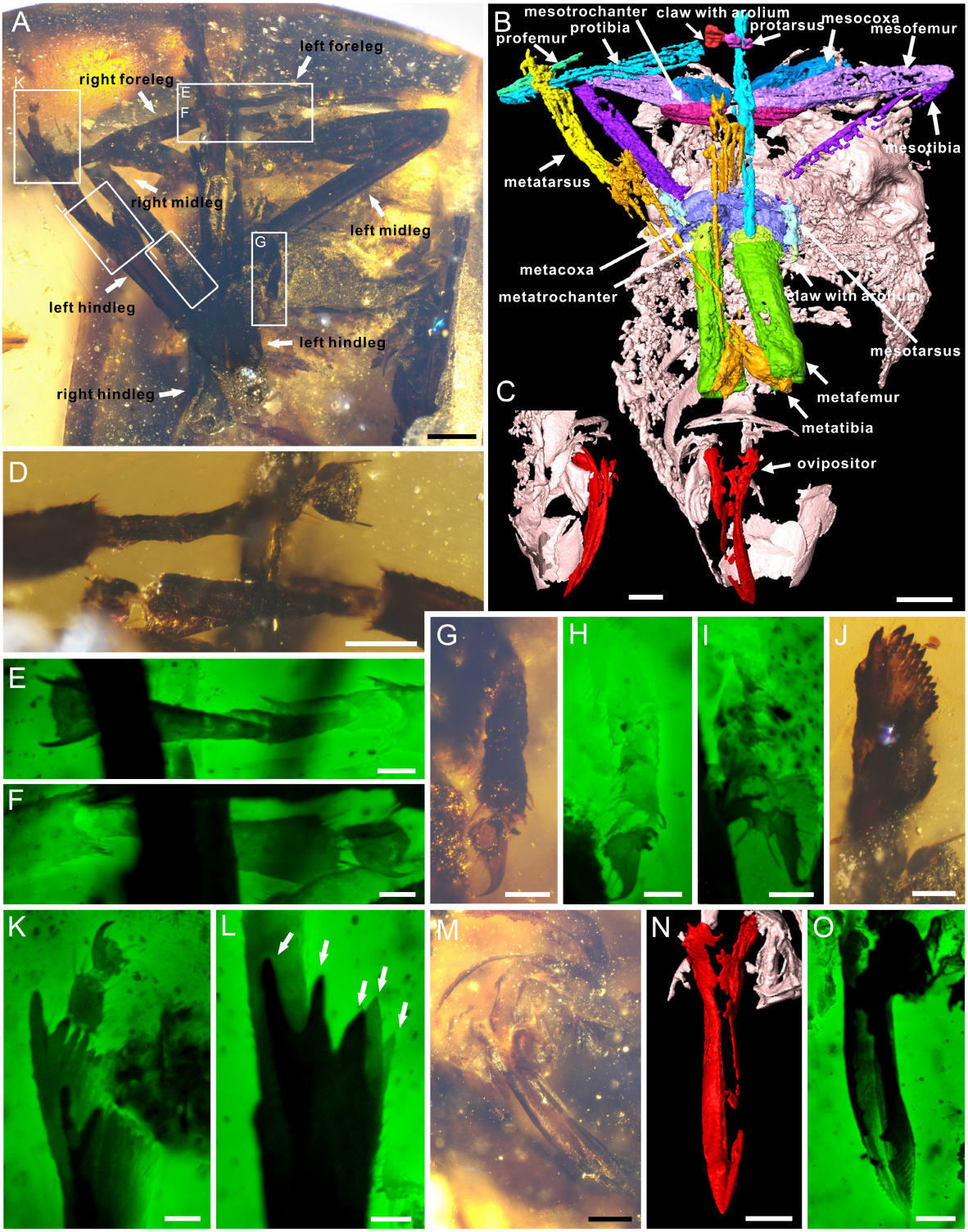

FIGURE 4. Body details of *Cretolala kachinensis* **gen. et sp. nov.**, holotype (HMJ–2016–019). **A**, Legs, overview, reflected-light micrograph. **B**, Legs, overview, micro-CT reconstruction. **C**, Female ovipositor, right lateral view, micro-CT reconstruction. **D**, Foreleg tarsus and pretarsus, dorsal view, reflected-light micrograph. **E**, Left foreleg tarsus and pretarsus, ventral view (from **A**), confocal laser scanning micrograph (CLSM). **F**, Right foreleg tarsus and pretarsus, ventral view (from **A**), CLSM. **G**, Left midleg tarsus and pretarsus, reflected-light micrograph. **H**, CLSM corresponding to **G**. **I**, Right midleg tarsus and pretarsus, CLSM. **J**, Right hind leg, tarsal apex bearing multiple spines, reflected-light micrograph. **K**, Left hind leg, tarsal apex with multiple spines and pretarsus, CLSM. **L**, Metatibia apex with five spines, CLSM. **M**–**O**, Female ovipositor: **M**, Reflected-light micrograph; **N**, Micro-CT reconstruction; **O**, CLSM. Scale bars = 0.4 mm (**A**); 0.5 mm (**B**–**D**); 100 µm (**E**, **F**, **H**, **I**, **K**, **L**); 0.1 mm (**G**, **J**, **M**); 0.25 mm (**N**); 200 µm (**O**).

Female terminalia (Fig. 4). Ovipositor well-developed, orthopteroid in type, with a relatively rounded tip, length about 1.5 mm, width about 0.2 mm. Distal portion with serrations of gonapophysis IX.

Preservation (Fig. 5). Reflected-light images show minerals in contact with and partially covering body structures (Fig. 5A, B). Micro-CT confirms the presence of pervasive mineral phases coatings on anatomical surfaces and occupying the body cavity, visible as bright, high-attenuation areas and mid-gray areas (Fig. 5C, D). SEM imaging, EDS mapping, and spot analyses identify quartz, feldspar (including both K-feldspar and Na-plagioclase), pyrite and aluminosilicate mineral mixtures as the principal body-coating and void-filling minerals (Fig. 5E–I).

In backscattered electron (BSE) images, pyrite occurs as bright, high-Z particles and aggregates, including isolated euhedral microcrystals, cavity-filling framboids with overgrowths, and blocky pyrite aggregates with overgrowths (Fig. 5E, F, I). Quartz occurs predominantly as granular infill, passing into blocky aggregates along cavity margins and around pyrite. Feldspar occurs as lath- to block-shaped crystals. EDS spectra and semi-quantitative analyses confirm the presence of K-feldspar (K-enriched) and Na-plagioclase (Na-enriched) (Fig. 5E, F, I). Some mineral aggregates occur as irregular patches with uneven surfaces and are confirmed by EDS spectra and semi-quantitative analyses as aluminosilicate mixtures, most probably clay minerals, characterized by Si–Al–dominated compositions with localized enrichment in K, Na, Mg, or Ca (Fig. 5F, I). Raman spectroscopy yielded no diagnostic mineral peaks due to fluorescence interference.

Discussion

The head and the dorsum of the thorax are not preserved; therefore, the taxonomic placement of the new specimen is based mainly on forewing morphology, supplemented by partially preserved leg and genitalic structures. The venation pattern of *Cretolala* **gen. nov.** conforms to the general venation scheme of Fulgoromorpha, and the fossil exhibits several conspicuous features, such as A_1 entering Pcu without first joining A_2, more than a dozen apical terminals in tegmen, a metatibial apex with multiple apical teeth, and a relatively high number of apical teeth on metatarsomeres (Bourgoin *et al*., 2015; Bucher *et al*., 2024). Based on the absence of an extravenal pterostigma, the presence of weakening in the stigmal area, the pattern of terminal branching of CuA in the tegmen, and the structure of the metathoracic legs, the fossil is best placed within the family Lalacidae (Bucher *et al*., 2024; Brożek *et al*., 2024).

Given the limited set of characters preserved in the fossil, the incomplete preservation of other described genera, and the need for a more comprehensive revision of the family based on better material, the information currently available precludes placement of *Cretolala* **gen. nov.** in any of the recognized subfamilies or tribes of Lalacidae. *Cretolala* **gen. nov.** lacks distinct subapical sarcochaetae and platellae on the metathoracic legs, a condition that clearly distinguishes it from Aptian Lalacidae known from the Crato Formation (Hamilton, 1990; Brożek *et al*., 2024). In terms of tegminal venation, the fossil shares more characters with Lalacidae from China, namely the Barremian genus *Lapicixius* and the Aptian genera *Cretocixius* and *Yanducixius*, yet it still differs from them in several distinct respects. For example, the tegmen of *Cretolala* **gen. nov.** has a narrow base and distinctly widened apical portion, resembling that of *Cretocixius* but differing from the elongate, not basally narrowed tegmina of *Yanducixius* and *Lapicixius*. The costal margin of *Cretolala* **gen. nov.** is strengthened and Pc+CP is shifted away from the anterior margin near the base, running parallel to CA and forming a narrow, sclerotized costal area, whereas in *Yanducixius* Pc+CP is simply parallel to the costal margin and in *Cretocixius* it is displaced more distally and not parallel to CA at the base. In *Cretolala* **gen. nov.**, ScP+R forks basad the CuA fork, whereas it forks more apicad in *Cretocixius* and *Lapicixius* and only slightly more basad in *Yanducixius*. The RP branch of *Cretolala* **gen. nov.** is basally curved and directed medially, as in *Lapicixius*, whereas in *Cretocixius* RP is straight and subparallel to the costal margin, and in *Yanducixius* it is basally curved and then subparallel to the costal margin. In *Cretolala* **gen. nov.**, CuA_2 forks slightly basad of the claval apex, as in *Lapicixius*, whereas in *Cretocixius* CuA_2 forks distinctly apicad of the claval apex, and in *Yanducixius* it forks slightly apicad of the claval apex. In *Cretolala* **gen. nov.**, the tornus is straight and aligned with the claval margin, in contrast to the tornus of *Cretocixius,* which sinuately diverging medially, and the slightly convex tornus of *Yanducixius* and *Lapicixius*.

Currently, 12 fulgoromorphan families have been documented from Burmese amber—four extant (Achilidae, Cixiidae, Derbidae, and Nogodinidae) and eight extinct families (Dorytocidae, Fulgoridiidae, Inoderbidae, Jubisentidae, Katlasidae, Mimarachnidae, Perforissidae, and Yetkhatidae) (Wang *et al*., 2025). The fossil described in this study, *Cretolala kachinensis* **gen. et sp. nov.**, is the first record of the family Lalacidae in amber from the Kachin region of northern Myanmar, and the first Cenomanian occurrence of this family.

In *Cretolala kachinensis* **gen. et sp. nov.**, wing maculation is preserved on the retained portions of the forewings and on the preserved distal part of the hind wing. Forewing maculation is widespread and diverse in

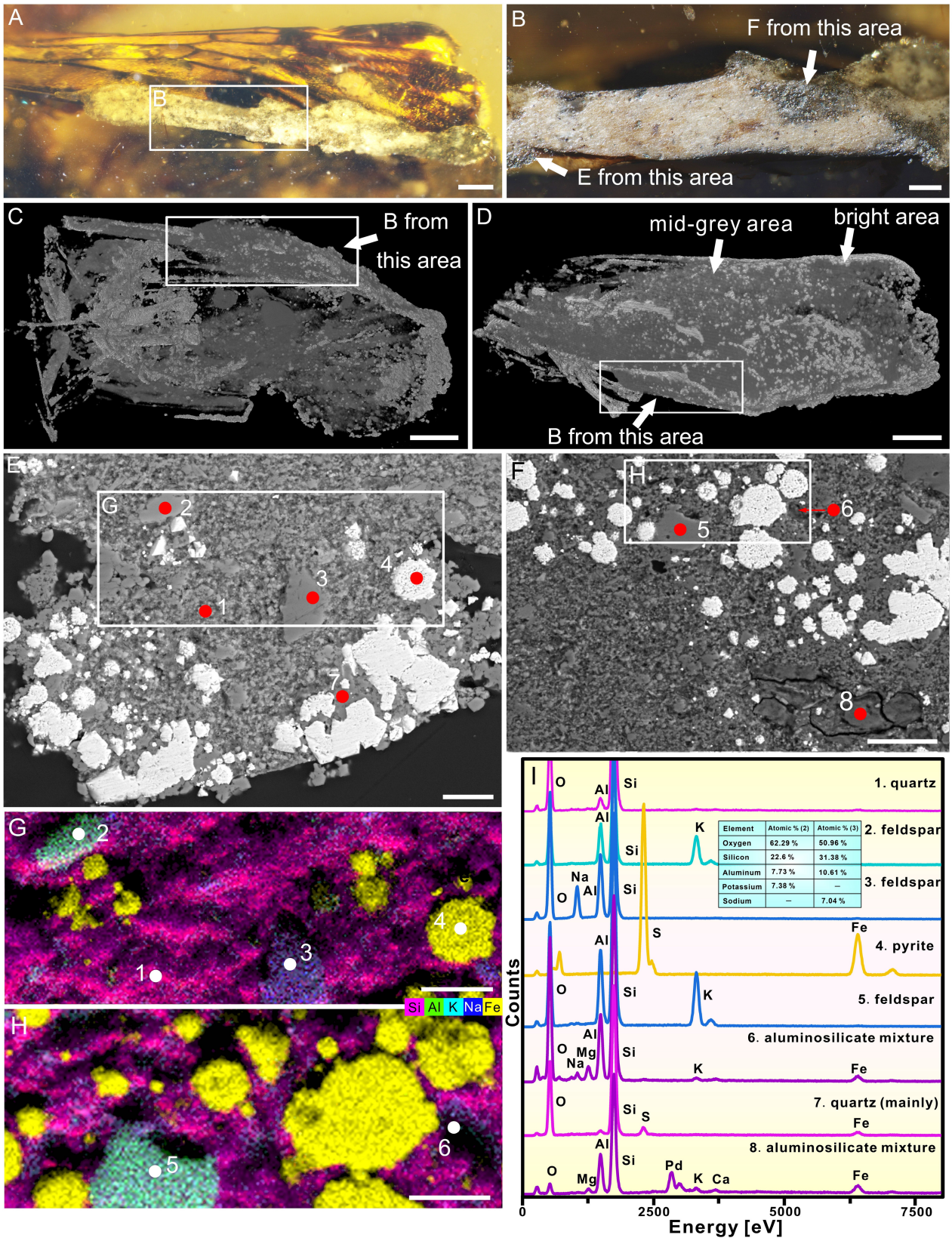

FIGURE 5. Taphonomic analysis of *Cretolala kachinensis* **gen. et sp. nov.**, HMJ–2016–019. **A**, **B**, Reflected-light micrographs of the same specimen; the boxed area in B was selected for SEM–EDS. **C**, **D**, Micro-CT reconstructions showing attenuation contrasts: bright areas (high attenuation); mid-grey areas (moderate attenuation). **E**, **F**, SEM–BSE images of the regions in **B**. Red points (1–8) indicate EDS spot analyses; the corresponding results are shown in **I**. **G**, **H**, Element map overlays for **E** and **F**. **I**, Representative EDS spectra for numbered spots corresponding to points in **E**–**H**. Scale bars = 1 mm (**A**, **B**), 0.5 mm (**C**), 0.2 mm (**D**), 25 μm (**E**), 50 μm (**F**), 20 μm (**G**, **H**).

Fulgoromorpha (Bourgoin, 2025: https://flow.hemiptera-databases.org/flow/). Insects display striking variation in coloration and patterning across species, populations, and individuals. These traits mediate diverse biological functions, including mate choice, recognition, mimicry, aposematism, deflection, and camouflage, and can also contribute to thermoregulation, photoprotection, and water balance (*e.g.*, Wittkopp *et al*., 2003; Parchem *et al*., 2007; Wittkopp & Beldade, 2009). Evidence indicates that color pattern evolution is not governed by a single selective regime, and the dominant ecological pressures vary across taxa, populations, environments, and evolutionary timescales (Wittkopp *et al*., 2003). In our specimen, the dorsal pattern forms a face-like arrangement (eye-like spots and a mouth-like element), suggesting possible aposematic or mimetic signaling, whereas the lateral outline may act as plant-like camouflage—plausible in an arboreal herbivore (Fig. 6). These ecological interpretations remain tentative but provide testable hypotheses for future comparative analyses of wing maculation in Lalacidae.

The new species exhibits a forewing maculation pattern distinct from that reported in other lalacid fossils (Fig. 2), thereby increasing the morphological disparity of fossil Lalacidae and providing new data for ecological inferences across fossil assemblages of Fulgoromorpha. Maculated forewings are widespread among cicadomorphans and fulgoromorphans, with groups tightly linked to their host plants. Recent diversification analyses have demonstrated that global floristic turnover impacted the evolutionary trajectories of these lineages (Boderau *et al*., 2025c). Quantitative analyses integrating fossils with well-preserved wing maculation and extant taxa remain to be undertaken. Such analyses will help clarify the paleoecological signal and selective pressures across clades and evolutionary timescales. However, this will also require more complete fossil material. Robust evolutionary inference emerges only when fossils from different intervals are compared with extant taxa using both wing and body characters (Jiang *et al*., 2024). Many Mesozoic specimens represent stem groups of extant lineages. The new material is incompletely preserved and lacks important structures such as the head and thorax. Additional specimens would help expand character sampling and further clarify patterns of morphological, phylogenetic, and ecological evolution.

The examination of the studied specimen give light about the state of preservation of the amber inclusion. Reflected-light results indicate the occurrence of mineral phases filling fractures around the specimen and are locally contiguous with wing structures. Using material-dependent X-ray attenuation in the micro-CT dataset, we mapped these phases throughout other body regions. The

FIGURE 6. Life reconstruction of *Cretolala kachinensis* **gen. et sp. nov.** (illustrated by Lucia Šmídová).

minerals primarily delineate and stabilize pre-existing cavities and spaces, enhancing attenuation contrast and improving reconstruction of soft-tissue in micro-CT reconstruction of insects trapped in Kachin amber, a result consistent with the interpretation of Stagg *et al*. (2026). In our specimen, these attenuation contrasts principally represent cavities and mineral infills rather than direct replacement of fine soft-tissue structures.

SEM-EDS shows K-feldspar and Na-plagioclase as blocky grains within a matrix of widespread fine-grained quartz. Pyrite occurs mainly as cavity-filling framboidal and blocky aggregates with euhedral overgrowths, locally surrounded by larger quartz crystals. Si–Al–dominated materials with variable enrichment in K, Na, Mg, or Ca, occur as micrometer-scale infillings and as larger, compact patches between fine quartz grains.

Based on the observed mineral assemblages and their textural relationships, we propose a tentative paragenetic model in which fine-grained quartz and feldspar entered the resin as detrital grains, infilling open cavities and voids, consistent with the mineralogy of the host sediments of Kachin amber (Cruickshank & Ko, 2003; Shi *et al*., 2012). Regarding the source of feldspar and fine-grained quartz, although contributions from authigenic silica or altered ash-derived aluminosilicates cannot be entirely ruled out, the angular grain shapes, blocky habits, and mineral associations support a detrital origin introduced by fluid infiltration. Pyrite then precipitated in pore spaces under sulfate-reducing conditions and later experienced overgrowths during subsequent fluid pulses. This was followed by precipitation of authigenic silica, forming large crystals and cavity-lining overgrowths. Aluminosilicate mixtures likely represent clay/silica aggregates derived from feldspar alteration and/or late-stage gel aggregation within the silica-rich matrix. The feldspar grains observed here likely reflect host-sediment input and indicate episodic communication between resin interiors and surrounding sediments.

Taphonomic studies of Kachin amber indicate that calcite, quartz, pyrite, and clay minerals are widely present within inclusions (*e.g*., Jiang *et al*., 2022; Stagg *et al*., 2026). Stagg *et al*. documented calcite, quartz, pyrite, and clay minerals co-occurring as infills within single body cavities in mayfly fossils from Kachin amber and proposed a tentative infilling sequence. They further analyzed the clay minerals, focusing on composition and implications for preservation in Kachin amber. In our specimen, calcite was not detected; instead, we identified feldspar (K-feldspar and Na-plagioclase) and fine-grained quartz occurring as detrital grains. This indicates that host-sediment material was introduced by fluids into voids within the amber (resin/copal), thereby contributing to cavity infilling and influencing preservation. Collectively, these observations support a multistage diagenetic history for Kachin amber and highlight variability among inclusions in mineral assemblages and timing. Recent work shows that sedimentary rock associated with amber affects its preservation (Lozano *et al*., 2025), potentially influencing the preservation of inclusions in other amber localities as well and warranting further investigation.

Conclusion

In this study, we describe *Cretolala kachinensis* **gen. et sp. nov.**, a new lalacid taxon from mid-Cretaceous Kachin amber, and provide an artistic reconstruction in Fig. 6. This fossil represents the first amber record of Lalacidae, the first Cenomanian record of this family, and adds a third fossil locality for Lalacidae in the Northern Hemisphere. The distinctive combination of venational and body features, together with the unique forewing maculation of *Cretolala kachinensis* **gen. et sp. nov.**, expands the known morphological diversity of Lalacidae and provides a first step toward refining the morphological concept of the family, while also offering new insights into its evolutionary history. At the same time, it highlights the need for additional, well-preserved material to refine the family's taxonomy further. In addition, our taphonomic analysis of *Cretolala kachinensis* **gen. et sp. nov.** indicates that preservation in Kachin amber is strongly influenced by mineral infilling. The specimen records a multistage diagenetic history, with variation in mineral assemblages and timing even among inclusions from the same deposits. These insights contribute to a more nuanced understanding of the conditions governing soft-tissue and morphological fidelity in Cretaceous amber faunas.

Acknowledgements

We thank the two reviewers for their constructive comments; the editors for handling the manuscript and assistance with the text; André Nel, Juan Diego Martín Martín, Ming Ma, Miguel López Blanco for helpful discussions; Xiaojing Liu for the initial analysis of wing venation. Funding was provided by the Deutsche Forschungsgemeinschaft (DFG) as a contribution to the DFG Research Unit FOR 2685, The Limits of the Fossil Record (publication #72), by the cooperation project between Charles University and the State Key Laboratory of Palaeobiology and Stratigraphy (No. 223114), and by the China Scholarship Council (CSC; 202307030030 to Y.-N.T.). M.B. contributed to this work during his Ph.D. thesis. C.J. was supported by the project CREI, PID2022-137316NB, of the Spanish MICIU (AEI) with FEDER funds. This publication was supported by the Open Access Publication Fund of the University of Bonn.

Data availability: All data generated or analysed during this study are included in this published article, or their sources are cited therein. The micro-CT data generated during the current study are available in Zenodo at [https://doi.org/10.5281/zenodo.19160691].

References

Boderau, M., Nel, A. & Fu, Y.Z. (2025a) A new *Lapicixius* planthopper species (Fulgoromorpha: Lalacidae) from the Lower Cretaceous Yixian Formation of northeastern China. *Journal of Insect Biodiversity*, 77 (1), 85–90. https://doi.org/10.12976/jib/2025.77.1.12

Boderau, M., Fu, Y.Z., Jiang, H., Guan, S., Peng, A., Nel, A. & Jouault, C. (2025b) Bayesian modelling of the fossil record enlightens the evolutionary history of Hemiptera. *Proceedings of the Royal Society B*, 292, 20251133. https://doi.org/10.1098/rspb.2025.1133

Boderau, M., Nel, A. & Jouault, C. (2025c) Diversification and extinction of Hemiptera in deep time. *Communications Biology*, 8 (1), 352. https://doi.org/10.1038/s42003-025-07773-x

Bourgoin, T. (1993) Female genitalia in Hemiptera Fulgoromorpha, morphological and phylogenetic data. *Annales de la Société entomologique de France, (N.S.)*, 29 (3), 225–244. https://doi.org/10.1080/21686351.1993.12277686

Bourgoin, T. (2025) FLOW (Fulgoromorpha Lists on The Web): a world knowledge base dedicated to Fulgoromorpha. Available from: https://flow.hemiptera-databases.org/flow/?&lang=en (accessed 30 Oct 2025).

Bourgoin, T. & Szwedo, J. (2022) Toward a new classification of planthoppers Hemiptera Fulgoromorpha: 1. What do Fulgoridiidae really cover? *Annales Zoologici*, 72 (4), 951–962. https://doi.org/10.3161/00034541ANZ2022.72.4.011

Bourgoin, T. & Szwedo, J. (2023) Toward a new classification of planthoppers Hemiptera Fulgoromorpha: 2. Higher taxa, their names and their composition. *Zootaxa*, 5297 (4), 562–568. https://doi.org/10.11646/zootaxa.5297.4.5

Bourgoin, T., Wang, R.R., Asche, M., Hoch, H., Soulier-Perkins, A., Stroiński, A., Yap, S. & Szwedo, J. (2015) From micropterism to hyperpterism: recognition strategy and standardized homology-driven terminology of the forewing venation patterns in planthoppers (Hemiptera: Fulgoromorpha). *Zoomorphology*, 134, 63–77. https://doi.org/10.1007/s00435-014-0243-6

Brożek, J., Stroiński, A., Romaniak, A. & Bourgoin, T. (2024) Disparity of metatibial and metatarsal cuticular and sensory structures in Cixiidae (Hemiptera: Fulgoromorpha) with a metatibiotarsal diagnosis for the tribes. *Zoological Letters*, 10 (1), 16. https://doi.org/10.1186/s40851-024-00239-8

Bucher, M. (2024) *Les grandes extinctions de masse ont-elles impacté l'évolution des insectes? Exemple de l'histoire macroévolutive des Hémiptères Fulgoromorpha. Systématique, phylogénie et taxonomie*. Thèse de doctorat, Museum national d'histoire naturelle (MNHN), Paris, 409 pp.

Bucher, M., Gignoux, G., Szwedo, J. & Bourgoin, T. (2024) Time-traveling through fossil planthopper tegmina in the Paleozoic and Mesozoic eras (Insecta: Hemiptera: Fulgoromorpha). *Palaeoentomology*, 7 (1), 1–67. https://doi.org/10.11646/palaeoentomology.7.1.1

Cruickshank, R.D. & Ko, K.O. (2003) Geology of an amber locality in the Hukawng Valley, Northern Myanmar. *Journal of Asian Earth Sciences*, 21 (5), 441–455. https://doi.org/10.1016/S1367-9120(02)00044-5

Hamilton, K.G.A. (1990) Insecta from the Santana Formation, Lower Cretaceous, of Brazil. Chapter 6. Homoptera. *Bulletin of the American Museum of Natural History*, 195, 82–122.

Haug, J.T., Azar, D., Ross, A.J., Szwedo, J., Wang, B., Arillo, A., Baranov, V., Bechteler, J., Beutel, R.G., Blagoderov, V., Delclòs, X., Feldberg, K., Feldmann, R., Foth, C., Fraaije, R.H.B., Gehler, A., Harms, D., Hedenäs, L., Hyžný, M., Jagt, J.W.M., Jagt-Yazykova, E.A., Jarzembowski, E.A., Kerp, H., Khine, P.K., Kirejtshuk, A.G., Klug, C., Kopylov, D.S., Kotthoff, U., Kriwet, J., McKellar, R.C., Nel, A., Nützel, A., Peñalver, E., Perrichot, V., Pint, A., Ragazzi, E., Regalado, L., Reich, M., Rikkinen, J., Schmidt, A.R., Schneider, H., Schram, F.R., Schweigert, G., Selden, P.A., Solórzano-Kraemer, M.M., Stilwell, J.D., van-Bakel, B.W.M., Vega, F.J., Wang, Y., Xing, L.D. & Haug, C. (2020) Comment on the letter of the Society of Vertebrate Paleontology (SVP) dated April 21, 2020, regarding "Fossils from conflict zones and reproducibility of fossil-based scientific data": Myanmar amber. *Paläontologische Zeitschrift*, 94, 431–437. https://doi.org/10.1007/s12542-020-00522-x

International Commission on Zoological Nomenclature (ICZN) (1999) *International code of zoological nomenclature*. Fourth Edition. International Trust for Zoological Nomenclature, London, xxix + 336 pp.

Jiang, H., Tomaschek, F., Muscente, A. D., Niu, C., Nyunt, T. T., Fang, Y., Schmidt, U., Chen, J., Lönartz, M., Mähler, B., Wappler, T., Jarzembowski, E.A., Szwedo, J., Zhang, H., Rust, J. & Wang, B. (2022) Widespread mineralization of soft-bodied insects in Cretaceous amber. *Geobiology*, 20, 363–376. https://doi.org/10.1111/gbi.12488

Jiang, H., Szwedo, J., Labandeira, C.C., Chen, J., Moulds, M.S., Mähler, B., Muscente, A.D., Zhuo, D., Nyunt, T.T., Zhang, H.C., Wei, C., Rust, J. & Wang, B. (2024) Mesozoic evolution of cicadas and their origins of vocalization and root feeding. *Nature Communications*, 15, 376. https://doi.org/10.1038/s41467-023-44446-x

Lozano, R.P., López Del Valle, R., Baeza, E., Delvene, G., Barrón, E., Peñalver, E., Rodrigo, A. & Pérez-de la Fuente, R. (2025) Preventive conservation of amber: some preliminary

investigations. Pyrite decay in amber: deterioration of collections and conservation guidelines. *Geoheritage*, 17 (4), 168.
https://doi.org/10.1007/s12371-025-01219-w

Nel, A., Prokop, J., Nel, P., Grandcolas, P., Huang, D.Y., Roques, P., Guilbert, E., Dostál, O. & Szwedo, J. (2012) Traits and evolution of wing venation pattern in paraneopteran insects. *Journal of Morphology*, 273 (5), 480–506.
https://doi.org/10.1002/jmor.11036

Parchem, R.J., Perry, M.W. & Patel, N.H. (2007) Patterns on the insect wing. *Current Opinion in Genetics and Development*, 17 (4), 300–308.
https://doi.org/10.1016/j.gde.2007.05.006

Ren, D., Lu, L.W., Guo, Z.G. & Ji, S.A. (1995) *Faunae and stratigraphy of Jurassic-Cretaceous in Beijing and the adjacent areas*. Seismic Publishing House, Beijing, viii+222 pp.

Ren, D., Yin, J. & Dou, W. (1998) New planthoppers and froghoppers from the Late Jurassic of northeast China (Homoptera: Auchenorrhyncha). *Acta Zootaxonomica Sinica*, 23 (3), 281–288.

Schubnel, T., Desutter-Grandcolas, L., Legendre, F., Prokop, J., Mazurier, A., Garrouste, R., Grandcolas, P. & Nel, A. (2019) To be or not to be: postcubital vein in insects revealed by microtomography. *Systematic Entomology*, 45 (2), 327–336.
https://doi.org/10.1111/syen.12399

Scotese, C.R., Vérard, C., Burgener, L., Elling, R.P. & Kocsis, A.T. (2025) The Cretaceous world: plate tectonics, palaeogeography and palaeoclimate. *Geological Society, London, Special Publications*, 544, 31–202.
https://doi.org/10.1144/SP544-2024-28

Shi, G.H., Grimaldi, D.A., Harlow, G.E., Wang, J., Wang, J., Yang, M.C., Lei, W.Y., Li, Q.L. & Li, X.H. (2012) Age constraint on Burmese amber based on U-Pb dating of zircons. *Cretaceous Research*, 37, 155–163.
https://doi.org/10.1016/j.cretres.2012.03.014

Stagg, N.A., Jiang, H., Tomaschek, F., Staniczek, A.H., Mähler, B., Bruthansová, J., Nyunt, T.T. & Godunko, R.J. (2026). Hidden taxonomic and taphonomic diversity revealed by mayflies (Ephemeroptera: Hexagenitidae) from mid-Cretaceous Kachin amber. *Scientific Reports* (in press).
https://doi.org/10.1038/s41598-026-46621-8

Szwedo, J. (2007) Fulgoromorpha: planthoppers. *In*: Martill D.M., Bechly, G. & Loveridge, R.F. (Eds), *The Crato fossil beds of Brazil: window into an ancient world*. Cambridge University Press, Cambridge, pp. 297–313.
https://doi.org/10.1017/CBO9780511535512.012

Szwedo, J., Bourgoin, T. & Lefebvre, F. (2004) *Fossil planthoppers (Hemiptera: Fulgoromorpha) of the world. An annotated catalogue with notes on Hemiptera classification*. Studio 1, Warsaw, 199 pp.

Szwedo, J., Wang, B., Soszyńska-Maj, A., Azar, D. & Ross, A.J. (2020) International Palaeoentomological Society statement. *Palaeoentomology*, 3 (3), 221–222.
https://doi.org/10.11646/palaeoentomology.3.3.1

Thu, K. & Zaw, K. (2017) Gem deposits of Myanmar. *Geological Society, London Memoirs*, 48, 497–529.
https://doi.org/10.1144/m48.23

Wang, L.N., Szwedo, J., Zhuo, D., Xiao, C.T. & Luo, C.H. (2025) Adding to the diversity of Katlasidae (Hemiptera: Fulgoromorpha: Fulgoridoidea)—a new genus and species from mid-Cretaceous Kachin amber of northern Myanmar. *Palaeontologia Electronica*, 28 (3), 1–15.
https://doi.org/10.26879/1575

Wittkopp, P.J., Carroll, S.B. & Kopp, A. (2003) Evolution in black and white: genetic control of pigment patterns in *Drosophila*. *Trends in Genetics*, 19 (9), 495–504.
https://doi.org/10.1016/S0168-9525(03)00194-X

Wittkopp, P.J. & Beldade, P. (2009) Development and evolution of insect pigmentation: genetic mechanisms and the potential consequences of pleiotropy. *Seminars in Cell & Developmental Biology*, 20 (1), 65–71.
https://doi.org/10.1016/j.semcdb.2008.10.002

Zhang, Z. (2002) New early Cretaceous lalacid from Jingxi Basin of Beijing, China (Homoptera: Fulgoroidea). *Acta Zootaxonomica Sinica*, 27 (1), 20–23.